On the Physical Meaning of the Model of Two Uncoupled Isotrops

Michel T. Ivrlač and Josef A. Nossek
Institute for Circuit Theory and Signal Processing
Technische Universität München, D-80333 Munich, Germany
email: {ivrlac, nossek}@tum.de

***Abstract*—From first principles, we show that two non-isotropic radiators with a specific and uniquely determined far-field pattern can be modeled consistently as two uncoupled isotropic radiators, provided one is willing to accept a non-linear distortion of the geometry. This shows that the, per se, non-physical model of uncoupled isotrops can have physical meaning in correctly describing the behavior of special non-isotropic radiators. The necessary distortion of geometry and its consequences are discussed.**

I. Introduction

A model of a system of at least two radiators must take into account the self- and mutual coupling of and between all radiators, in order to be consistent with physical law [1]. Therefore, considering two isotropic radiators as being uncoupled does not correctly model the behavior of two real isotropic radiators. Yet, such a model may still describe correctly the behavior of a different system: namely two *non*-isotropic radiators cascaded with a lossless linear matching four-port. It turns out that this is indeed possible, provided the far-field pattern of the non-isotropic radiators is chosen properly. However, one has to accept a certain discrepancy between the distances and angles within the model of the uncoupled isotrops on the one hand, and the real system of the non-isotropic and, of course, coupled radiators, on the other.

It might be noted that the model of uncoupled isotrops is widespread in signal processing and information theory (see, e.g., [2]). Yet, that this model does *not* describe isotropic radiators at all, but rather two *non*-isotropic radiators with *distorted* geometry appears to have been overlooked. In the following, we first summarize our key results before deriving them.

II. Main Results

Consider two non-isotropic radiators in free space as shown in Figure 1. The radiated power P_{rad}, and received power P_{rec} in a point P well in the far-field in direction θ are given by:

$$P_{\text{rad}} \sim \boldsymbol{i}_{\text{A}}^{\text{H}} \boldsymbol{A} \boldsymbol{i}_{\text{A}}, \quad P_{\text{rec}} \sim \left| \boldsymbol{i}_{\text{A}}^{\text{T}} \boldsymbol{a}(\theta) \right|^2, \quad \boldsymbol{a}(\theta) = g(\theta) \begin{bmatrix} 1 \\ \mathrm{e}^{-\mathrm{j}kd\cos\theta} \end{bmatrix}. \tag{1}$$

Herein the superscripts $^{\text{T}}$ and $^{\text{H}}$ denote the transposition and the complex conjugated transposition, respectively. Moreover, $\boldsymbol{i}_A = [i_{\text{A},1}\ i_{\text{A},2}]^{\text{T}}$ is the vector of complex excitation current envelopes, and $\boldsymbol{a}(\theta)$ the array steering vector, while d denotes the separation between the two non-isotropic antennas, and $|g(\theta)|^2$ is their beam-pattern, which we assume depends on θ only. As usual, $k = 2\pi/\lambda$ denotes the wavenumber, with λ being the wavelength. The real and symmetric matrix $\boldsymbol{A}$ is a result of the mutual antenna coupling, and depends on the beam-pattern $|g(\theta)|^2$ and the distance d. Let us now assume

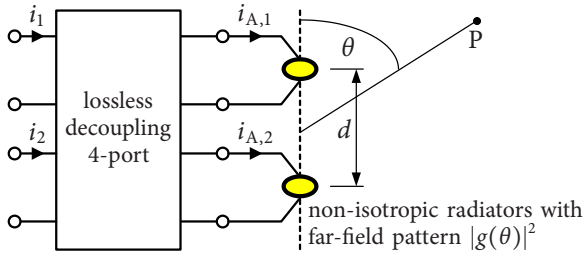

Figure 1: Array of two non-isotropic radiators with lossless decoupling 4-port, and point P in far-field.

that two ports of a loss-less linear decoupling four-port are connected to the antennas' excitation ports. By treating the remaining two ports as the excitation ports of a *virtual* array with complex excitation current envelopes i_1 and i_2, we can show that (1) can be written equivalently as:

$$P_{\text{rad}} \sim \boldsymbol{i}^{\text{H}} \boldsymbol{i}, \quad P_{\text{rec}} \sim \left| \boldsymbol{i}^{\text{T}} \boldsymbol{a}'(\theta') \right|^2, \quad \boldsymbol{a}'(\theta') = \begin{bmatrix} 1 \\ \mathrm{e}^{-\mathrm{j}kd'\cos\theta'} \end{bmatrix}, \tag{2}$$

where $\boldsymbol{i} = [i_1\ i_2]^{\text{T}}$. Note that (2) describes two *uncoupled* and *isotropic* radiators, which are placed a distance d' apart, and where the direction angle to the point P in the far-field is θ', for which holds the following non-linear relationship:

$$\cos\theta' = \frac{1}{kd'} \arg\left(\frac{\mathrm{e}^{-\mathrm{j}kd\cos\theta} - \zeta}{1 - \zeta \mathrm{e}^{-\mathrm{j}kd\cos\theta}} \right), \tag{3}$$

where ζ is only zero when d is an integer multiple of half the wavelength, and otherwise is the non-zero root of

$$\tan\left(\frac{1+\zeta^2}{1-\zeta^2} \cdot \frac{kd}{2} \right) + \frac{\zeta+1}{\zeta-1} \tan\frac{kd}{2} \tag{4}$$

in the interval $(-1, 1)$. Because θ' must be real-valued, it follows from (3) that d' cannot be allowed to be too small:

$$d' \geq \tau\lambda/2\pi, \quad \text{where } 2\arctan(\tau) = \tau, \quad \text{and } \tau > 0, \tag{5}$$

is *necessary* for θ' to be real-valued for all real θ. Since $\tau > 2.33$, it follows that, in no circumstance, the distance d' may drop below 0.37λ. In other words, if $d' \leq 0.37\lambda$, there is no far-field pattern $|g(\theta)|^2$ to make (2) equivalent with (1). Thus, the right far-field pattern $|g(\theta)|^2$ either does not exist (when d' is too small), or otherwise, as it turns out, is uniquely given by:

$$|g(\theta)|^2 = \frac{1-\zeta^2}{1+\zeta^2} \frac{1-\zeta^2}{1+\zeta^2-2\zeta\cos(kd\cos\theta)}. \tag{6}$$

In summary, two radiators with far-field patterns given by (6) can be modeled as two uncoupled isotrops provided one obeys the non-linear relationship (3) of geometric angles.

III. Mutual Antenna Coupling

When there flows an electric current with complex envelope i_A at the excitation port of a thin wire antenna, it excites, in a point P well in the far-field, an electric field strength which is proportional to $|i_A \cdot g(\theta,\phi)e^{-jkr}/r|$ (see e.g., [3], page 135) where r is the distance of P to the antenna (assumed large compared to the wavelength and the size of the antenna) and $g(\theta,\phi)$ is an antenna-dependent function of the elevation and azimuthal angles at which the antenna sees the point P. The constant j is the imaginary unit, i.e. $j^2 = -1$. In the following we assume for simplicity, that $g(\theta,\phi) = g(\theta)$, so that there is only dependence on one angle (θ). When two such antennas are placed in the same orientation a distance d apart, and excited with possibly different currents of complex envelopes $i_{A,1}$ and $i_{A,2}$, the resulting electric field is a superposition of the two individual fields. In the point P, the electric field strength $\mathcal{E}$ is proportional to $|i_{A,1}g(\theta)e^{-jkr}/r + i_{A,2}g(\theta)e^{-jkr'}/r'|$, where r and r' are the respective distances of P to the first and second antenna. Thus,

$$\mathcal{E} \sim \frac{|g(\theta)|}{r} \cdot \left| i_{A,1} + i_{A,2}\frac{r}{r'}e^{-jk(r'-r)} \right|. \tag{7}$$

When θ is defined as in Figure 1, then $r' \approx r + d\cos\theta$. Thus, for $r \gg d$ there is $r/r' \approx 1$, and (7) turns into

$$\mathcal{E} = \alpha\frac{|g(\theta)|}{r} \cdot \left| i_{A,1} + i_{A,2}e^{-jkd\cos\theta} \right| = \alpha\left|\boldsymbol{i}_A^T\boldsymbol{a}(\theta)\right|/r, \tag{8}$$

where we have introduced the antenna-specific constant factor α, and the antenna excitation current vector $\boldsymbol{i}_A = [i_{A,1}\ i_{A,2}]^T$, while the array steering vector $\boldsymbol{a}(\theta)$ was already defined in (1). Because the power density (power per unit area) in the far-field is proportional to the square of the electric field strength it holds for the power P_{rad} which is radiated by the antenna:

$$P_{rad} \sim \int_{\substack{\text{closed surface}\\ \text{around array}\\ \text{in far-field}}} \mathcal{E}^2 \mathrm{d}A. \tag{9}$$

It is easiest to integrate over the surface of a sphere which contains both antennas and which radius is large enough such that its surface is well in the far-field. From (8) and (9) we thus obtain

$$P_{rad} \sim \boldsymbol{i}_A^T\boldsymbol{A}\boldsymbol{i}_A^*, \quad \text{where } \boldsymbol{A} = \int_0^\pi \boldsymbol{a}(\theta)\boldsymbol{a}^H(\theta)\sin(\theta)\mathrm{d}\theta, \tag{10}$$

where * denotes complex conjugation. Clearly, $\boldsymbol{A} = \boldsymbol{A}^H$, so that P_{rad} is real-valued, as it must be. Thus, one can also write $P_{rad} \sim \boldsymbol{i}_A^H\boldsymbol{A}^*\boldsymbol{i}_A$, or

$$P_{rad} = R\,\boldsymbol{i}_A^H\begin{bmatrix}1 & a\\ a & 1\end{bmatrix}\boldsymbol{i}_A, \quad R > 0, \tag{11}$$

with a properly chosen, real-valued and positive factor $R > 0$ of proportionality. By substituting the definition of $\boldsymbol{a}(\theta)$ from (1) into (10), it follows with the help of (11) that the *mutual coupling coefficient*, a, depends on the *beam-pattern*, $|g(\theta)|^2$, of the two individual antennas, as well as on their *distance*, d:

$$a = \frac{\int_0^\pi |g(\theta)|^2\cos(kd\cos\theta)\sin(\theta)\mathrm{d}\theta}{\int_0^\pi |g(\theta)|^2\sin(\theta)\mathrm{d}\theta}. \tag{12}$$

Note that a is real-valued, and furthermore

$$-1 \le a \le 1, \tag{13}$$

such that $P_{rad} \ge 0$ for *every* excitation vector $\boldsymbol{i}_A$ is granted.

IV. Virtual Array of Uncoupled Isotrops

Now let us assume we connect the two ports of the antenna array to two ports of a *loss-less* linear 4-port, which is designed such that its other two ports then become electrically *decoupled* and look like resistances of value $R > 0$. This setup is shown in Figure 1. If we call $\boldsymbol{i} = [i_1\ i_2]^T$ the vector of the port currents of these two decoupled ports, then the power entering the 4-port through these two ports is given by:

$$P_{in} = R|i_1|^2 + R|i_2|^2 = R\,\boldsymbol{i}^H\boldsymbol{i}. \tag{14}$$

Since the 4-port is loss-less, this power must leave through the other 2 ports and flow into the antenna array. Assuming the antennas have no heat-loss either, the power P_{in} is radiated:

$$P_{rad} = P_{in} = R\,\boldsymbol{i}^H\boldsymbol{i} = R\,\boldsymbol{i}_A^H\begin{bmatrix}1 & a\\ a & 1\end{bmatrix}\boldsymbol{i}_A. \tag{15}$$

This is a nice property, because the radiated power is proportional to the squared Euclidean norm of $\boldsymbol{i}$, for every distance d of the antennas, and every beam pattern $|g(\theta)|^2$. Because the 4-port is linear, the relationship between $\boldsymbol{i}$ and $\boldsymbol{i}_A$ is linear:

$$\boldsymbol{i}_A = \boldsymbol{T}\boldsymbol{i}, \tag{16}$$

where $\boldsymbol{T} \in \mathbb{C}^{2\times 2}$. Substituting (16) into (15), it follows that

$$\boldsymbol{T} = \begin{bmatrix}1 & a\\ a & 1\end{bmatrix}^{-1/2}\boldsymbol{Q}, \qquad \text{where } \boldsymbol{Q}\boldsymbol{Q}^H = \boldsymbol{Q}^H\boldsymbol{Q} = \mathbf{I}_2. \tag{17}$$

Recalling (8), the electric field strength in a point in the far-field was given by $\mathcal{E} = \alpha\left|\boldsymbol{i}_A^T\boldsymbol{a}(\theta)\right|/r$. Now it would be nice, if the same electric field strength could be expressed by

$$\mathcal{E} = \alpha\left|\boldsymbol{i}^T\boldsymbol{a}'(\theta')\right|/r, \quad \text{where } \boldsymbol{a}'(\theta') = \gamma\begin{bmatrix}1\\ e^{-jkd'\cos\theta'}\end{bmatrix}, \tag{18}$$

where γ is a suitably chosen *constant*. Notice that the vector $\boldsymbol{a}'$ is the steering vector of an array of two *isotropic* radiators which are spaced a distance d' apart (which my be different from d). Moreover, the angle between the axis of this array of isotrops and the radius vector to a point P in space is called θ', which may be different from θ. Therefore, it is proper to say that the decoupling 4-port presents us with a *virtual* array of isotrops, that may require a *distorted geometry* in the sense that the angle θ' may be substantially different from the angle θ which we use for the real array of non-isotropic antennas in Figure 1. Because of the action of the loss-less decoupling 4-port, the two isotrops of this virtual array act as if uncoupled,

independent of the value of the virtual distance d', or even the real distance d. In summary, we can say that the decoupling network provides a virtual array which is mathematically exactly described as an array of two uncoupled isotrops. In the following we will see that this requires a special relationship between the angles θ' and θ, as well as a very specific beampattern $|g(\theta)|^2$ of the real individual antennas.

V. The Beampattern

Comparing (8) and (18), we see that $\boldsymbol{i}_{\mathrm{A}}^{\mathrm{T}}\boldsymbol{a}(\theta) = \boldsymbol{i}^{\mathrm{T}}\boldsymbol{a}'(\theta')$ must hold (up to a unimodular factor, which one can absorb into γ in (18)). With the help of (16) it therefore follows that

$$\begin{bmatrix} 1 \\ \mathrm{e}^{-\mathrm{j}kd\cos\theta} \end{bmatrix} g(\theta) \;=\; \gamma \boldsymbol{T}^{-\mathrm{T}} \begin{bmatrix} 1 \\ \mathrm{e}^{-\mathrm{j}kd'\cos\theta'} \end{bmatrix}. \tag{19}$$

To simplify the notation, let us define:

$$\varphi = -kd\cos\theta, \quad \mu = -kd'\cos\theta', \quad \varphi, \mu \in \mathbb{R}. \tag{20}$$

Then, (19) is re-written as:

$$\begin{bmatrix} 1 \\ \mathrm{e}^{\mathrm{j}\varphi} \end{bmatrix} \tilde{g}(\varphi) \;=\; \underbrace{\begin{bmatrix} A & B \\ C & D \end{bmatrix}}_{\gamma \boldsymbol{T}^{-\mathrm{T}}} \begin{bmatrix} 1 \\ \mathrm{e}^{\mathrm{j}\mu} \end{bmatrix}, \tag{21}$$

where we have written the matrix $\gamma\boldsymbol{T}^{-\mathrm{T}}$ in terms of its four components (A, B, C, and D), and where

$$\tilde{g}(\varphi) = g\Big(\arccos\big(-\varphi/(kd)\big)\Big). \tag{22}$$

By dividing the second line of (21) by its first line, we see that:

$$\left|\frac{C + D\mathrm{e}^{\mathrm{j}\mu}}{A + B\mathrm{e}^{\mathrm{j}\mu}}\right| \;=\; 1, \quad \forall \mu \in \mathbb{R}. \tag{23}$$

This must hold for *every real-valued* μ. Let us write

$$\frac{C + D\mathrm{e}^{\mathrm{j}\mu}}{A + B\mathrm{e}^{\mathrm{j}\mu}} = \frac{C}{A} \cdot \frac{1 + \eta\mathrm{e}^{\mathrm{j}\mu}}{1 + \xi\mathrm{e}^{\mathrm{j}\mu}}, \quad \text{where } \eta = D/C, \quad \xi = B/A. \tag{24}$$

In order that (23) can hold true, we must have

$$\left|\frac{1 + \eta\mathrm{e}^{\mathrm{j}\mu}}{1 + \xi\mathrm{e}^{\mathrm{j}\mu}}\right| = K = \text{const}, \quad \forall \mu \in \mathbb{R},$$

which can be written alternatively as:

$$\begin{aligned} 1 + |\eta|^2 + 2|\eta|\cos\big(\mu + \mathrm{angle}(\eta)\big) \;=\; \\ K^2\left(1 + |\xi|^2 + 2|\xi|\cos\big(\mu + \mathrm{angle}(\xi)\big)\right), \quad \forall \mu \in \mathbb{R}. \end{aligned} \tag{25}$$

Since the cosine terms on each side of the equality must cancel, we must have $\mathrm{angle}(\eta) = \mathrm{angle}(\xi)$, and $|\eta| = K^2|\xi|$. Substituting these relationships into (25), we find that

$$K^4 - K^2\left(1 + |\eta|^2\right) + |\eta|^2 = 0, \tag{26}$$

must hold. This is a quadratic equation in K^2, which yields the two solutions: $K_1^2 = 1$, and $K_2^2 = |\eta|^2$. Recalling $|\eta| = K^2|\xi|$, and $\mathrm{angle}(\eta) = \mathrm{angle}(\xi)$, there are, thus, two possible relationships between η and ξ, such that (25) holds true: either $\eta = \xi$, or $\eta = 1/\xi^*$. The first solution means that $B/A = D/C$. However, this implies that the two rows of $\gamma\boldsymbol{T}^{-\mathrm{T}}$ are linearly dependent. Thus, $\gamma\boldsymbol{T}^{-\mathrm{T}}$ cannot be inverted and the electric current transformation matrix $\boldsymbol{T}$ is incomputable. Therefore, the *only feasible* solution is given by $\eta = 1/\xi^*$. Using this in (24) we find:

$$\frac{C + D\mathrm{e}^{\mathrm{j}\mu}}{A + B\mathrm{e}^{\mathrm{j}\mu}} = \frac{C}{A\xi^*} \cdot \frac{\xi^* + \mathrm{e}^{\mathrm{j}\mu}}{1 + \xi\mathrm{e}^{\mathrm{j}\mu}}. \tag{27}$$

As $|\xi^* + \mathrm{e}^{\mathrm{j}\mu}|/|1 + \xi\mathrm{e}^{\mathrm{j}\mu}| = 1$, for all μ, (23) requires:

$$\frac{C + D\mathrm{e}^{\mathrm{j}\mu}}{A + B\mathrm{e}^{\mathrm{j}\mu}} = \mathrm{e}^{\mathrm{j}\alpha} \cdot \frac{\xi^* + \mathrm{e}^{\mathrm{j}\mu}}{1 + \xi\mathrm{e}^{\mathrm{j}\mu}}, \quad \text{where } \alpha \in \mathbb{R}, \quad \xi \in \mathbb{C}. \tag{28}$$

From this follows that

$$\gamma\boldsymbol{T}^{-\mathrm{T}} = A\begin{bmatrix} 1 & \xi \\ \xi^*\mathrm{e}^{\mathrm{j}\alpha} & \mathrm{e}^{\mathrm{j}\alpha} \end{bmatrix}, \quad \text{where } A \in \mathbb{C} \tag{29}$$

is an arbitrary complex constant. Now let use define:

$$\zeta = \xi\mathrm{e}^{-\mathrm{j}\alpha}. \tag{30}$$

Because $|\zeta| = |\xi|$, the Gramian of (29) computes to

$$|\gamma|^2\boldsymbol{T}^{-\mathrm{T}}\boldsymbol{T}^{-*} = |A|^2\left(1 + |\zeta|^2\right)\begin{bmatrix} 1 & 2\zeta/(1+|\zeta|^2) \\ 2\zeta^*/(1+|\zeta|^2) & 1 \end{bmatrix}. \tag{31}$$

On the other hand, from (17), we obtain

$$|\gamma|^2\boldsymbol{T}^{-\mathrm{T}}\boldsymbol{T}^{-*} = |\gamma|^2\begin{bmatrix} 1 & a \\ a & 1 \end{bmatrix}. \tag{32}$$

By comparing (31) with (32), it follows that

$$\zeta \in \mathbb{R}, \quad |\gamma|^2 = |A|^2\left(1 + \zeta^2\right), \quad a = \frac{2\zeta}{1 + \zeta^2}. \tag{33}$$

The last equation for a is going to play a key role later, because it relates the *logical* parameter ζ with the *physical* parameter a (the mutual coupling coefficient). From (29), (30) and (33), the electric current transformation matrix $\boldsymbol{T}$ follows as:

$$\boldsymbol{T} = \mathrm{e}^{\mathrm{j}\beta}\frac{\sqrt{1+\zeta^2}}{1-\zeta^2}\begin{bmatrix} 1 & -\zeta\mathrm{e}^{-\mathrm{j}\alpha} \\ -\zeta & \mathrm{e}^{-\mathrm{j}\alpha} \end{bmatrix}, \quad \text{where} \quad \alpha, \beta, \zeta \in \mathbb{R}. \tag{34}$$

Note from (34) that the matrix $\boldsymbol{T}$ does *not* depend on the parameter A from (29). Therefore, we may set it to a convenient value. It will become clear later that

$$A = \frac{1}{\sqrt{1+\zeta^2}}, \tag{35}$$

is a reasonable choice. With (33) this implies that

$$|\gamma| = 1. \tag{36}$$

With (29), (30) and (35), we can re-write (21) as:

$$\begin{bmatrix} 1 \\ \mathrm{e}^{\mathrm{j}\varphi} \end{bmatrix} \tilde{g}(\varphi) = \frac{1}{\sqrt{1+\zeta^2}}\begin{bmatrix} 1 & \zeta \\ \zeta & 1 \end{bmatrix}\begin{bmatrix} 1 \\ \mathrm{e}^{\mathrm{j}(\mu+\alpha)} \end{bmatrix}, \quad \text{where } \alpha, \zeta \in \mathbb{R}. \tag{37}$$

When we divide the second line of (37) by its first line, we obtain: $\mathrm{e}^{\mathrm{j}\varphi} = (\zeta + \mathrm{e}^{\mathrm{j}(\mu+\alpha)})/(1 + \zeta\mathrm{e}^{\mathrm{j}(\mu+\alpha)})$. Thus,

$$\mathrm{e}^{\mathrm{j}(\mu+\alpha)} = \frac{\mathrm{e}^{\mathrm{j}\varphi} - \zeta}{1 - \zeta\mathrm{e}^{\mathrm{j}\varphi}}. \tag{38}$$

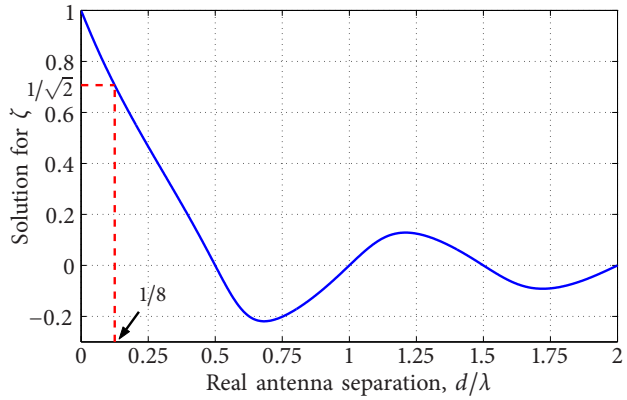

Figure 2: Numerical solution of (42).

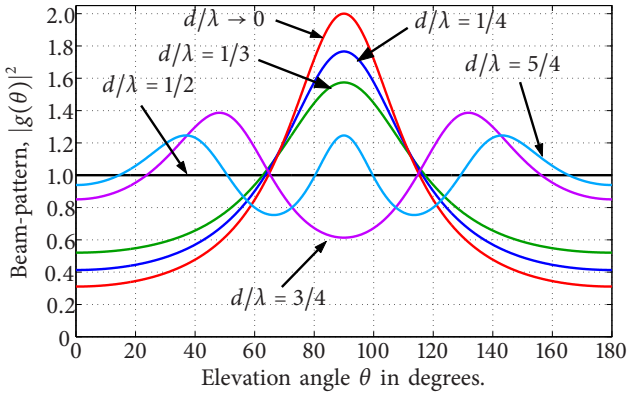

Figure 3: Beam-pattern of the real antennas.

The first line of (37) therefore becomes:

$$\tilde{g}(\varphi) = \frac{1}{\sqrt{1+\zeta^2}} \cdot \frac{1-\zeta^2}{1-\zeta e^{j\varphi}}. \tag{39}$$

Recalling (20) and (22), it follows from (39):

$$|g(\theta)|^2 = \frac{1-\zeta^2}{1+\zeta^2} \cdot \frac{1-\zeta^2}{1+\zeta^2-2\zeta\cos(kd\cos\theta)}. \tag{40}$$

This is the desired beam pattern of each of the real individual antennas. It depends, besides on kd, on the logical parameter ζ. *It has the property that it does* not *change when* ζ *is replaced by* $1/\zeta$. This property will come in handy later and is a consequence of our choosing the value of A according to (35). Now let us substitute (40) into (12) and carry out the integrations.

$$a = \frac{1+\zeta^2}{2\zeta} + \frac{(1-\zeta^2)\,kd}{4\zeta \arctan\left(\frac{\zeta+1}{\zeta-1}\tan\frac{kd}{2}\right)}. \tag{41}$$

Note that (41) does *not* depend on the specific choice of A that we have made in (35). This is because A only enters as a scaling factor into the beam-pattern $|g(\theta)|^2$, and therefore cancels out in (12). The result (41) is therefore independent of our particular choice of A in (35). Now (41) is not the only equation we have for a. In (33) we have already obtained another one. By equating the right hand side of the right-most equation in (33) with the right hand side of (41), we find the key equation for obtaining the possible values for ζ:

$$\tan\left(\frac{1+\zeta^2}{1-\zeta^2}\cdot\frac{kd}{2}\right) + \frac{\zeta+1}{\zeta-1}\tan\frac{kd}{2} = 0. \tag{42}$$

Because $\tan(-x) = -\tan(x)$, it is true that replacing ζ by $1/\zeta$ in (42) leaves the equation *unchanged*. Consequently, if ζ is a solution of (42), then so is also $1/\zeta$. Because the beam-pattern (40) is also not changed by replacing ζ with $1/\zeta$, both solutions for ζ are equivalent! Without loss of generality, we may therefore restrict the range of ζ to:

$$-1 \le \zeta \le 1. \tag{43}$$

A trivial solution is $\zeta = 0$. However, from (33) we see that this implies that the mutual coupling coefficient $a = 0$. In general, however, the mutual coupling coefficient is not going to be zero, so that we need to look for another solution of (42) in these cases. Fortunately, there exists another solution but it appears to refuse analytical treatment, except in certain special cases. For example, if $kd = \pi/4$, one finds that $\zeta = 1/\sqrt{2}$, *exactly*. In general though, one must resort to numerical computation, the result of which is displayed in Figure 2 as a function of the electrical distance d/λ between the two real antennas (recall $k = 2\pi/\lambda$ with λ being the wavelength). Note that $\zeta = 0$ only happens when d is an integer multiple of half the wavelength, or in the limit as $d/\lambda \to \infty$. As the electrical distance between the real antennas approaches zero, the value of ζ approaches unity from below. For small values of kd, one can find the asymptotic solution by guessing from Figure 2 that

$$\zeta \to 1 - kd/\tau, \quad \text{as } kd \to 0, \tag{44}$$

with a suitably chosen parameter τ which one finds by substituting $1 - kd/\tau$ for ζ in (42) and taking the limit $kd \to 0$:

$$\tan(\tau/2) - \tau = 0. \tag{45}$$

Despite appearance, it is difficult to solve for τ. Numerically,

$$\tau = 2.33112237041442261366\ldots. \tag{46}$$

Figure 3 shows the beam-patterns $|g(\theta)|^2$ which result from using the solutions ζ from Figure 2 for different distances d in (40). For d being an integer multiple of half the wavelength, the pattern is isotropic. A narrower spacing than half the wavelength makes the beam-pattern peak in the front-fire direction ($\theta = 90°$). For larger spacing than $\lambda/2$, the beam-pattern have got several peaks.

The *directivity* D of the beam-pattern is defined as the ratio of the maximum value of $|g(\theta)|^2$ and its average value over the unit sphere:

$$D = \frac{\max\limits_{\theta} |g(\theta)|^2}{\frac{1}{4\pi}\int_{\phi=0}^{2\pi}\int_{\theta=0}^{\pi} |g(\theta)|^2 \sin(\theta)\,d\theta\,d\phi}. \tag{47}$$

With ζ being a solution of (42) it can be shown that

$$D = \max_{\theta} |g(\theta)|^2. \tag{48}$$

This shows once more that our choice of A in (35) is convenient because it scales the beam-pattern just in the right way to show the directivity in its maximum value.

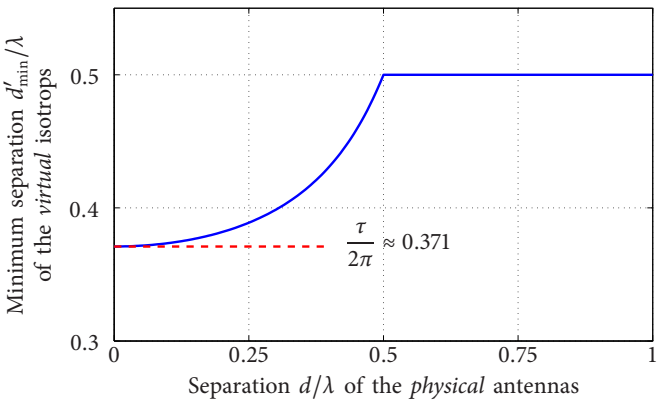

Figure 4: The minimum allowable separation $d'_{\min}/\lambda$ of the two *virtual* isotrops. In no circumstance can d' be allowed to be smaller than 0.371λ.

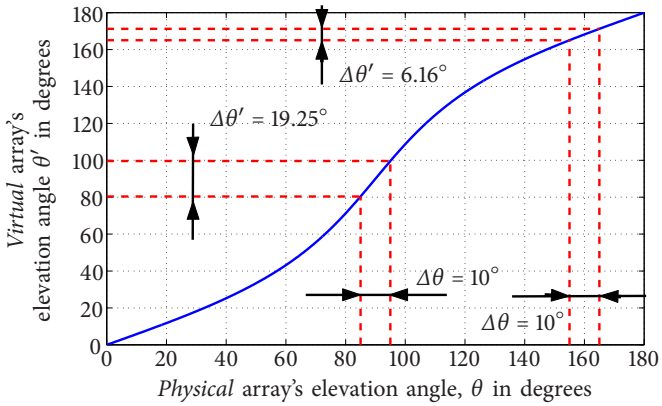

Figure 5: The relationship between the elevation angles perceived by the physical array and the virtual array for $d = \lambda/8$ and $d' = 3\lambda/8$.

VI. Distorted Geometry

Now that we know the beam-pattern of the real antennas, let us come back to the question of the relationship between the elevation angle θ of the real array, and the virtual elevation angle θ' that we must use in (18) such that it yields the same result as (8). We can find this relationship immediately when we substitute (20) into (38) and solve for θ':

$$\theta' = \arccos\left(\frac{\alpha}{kd'} + \frac{\mathrm{j}}{kd'}\ln\left(\frac{\mathrm{e}^{-\mathrm{j}kd\cos\theta} - \zeta}{1 - \zeta\mathrm{e}^{-\mathrm{j}kd\cos\theta}}\right)\right), \tag{49}$$

where $\alpha \in [-\pi, \pi]$. Note that:

$$\mathrm{j}\ln\left(\frac{\mathrm{e}^{-\mathrm{j}kd\cos\theta} - \zeta}{1 - \zeta\mathrm{e}^{-\mathrm{j}kd\cos\theta}}\right) = -\mathrm{angle}\left(\frac{\mathrm{e}^{-\mathrm{j}kd\cos\theta} - \zeta}{1 - \zeta\mathrm{e}^{-\mathrm{j}kd\cos\theta}}\right) \in [-\pi, \pi]. \tag{50}$$

Because θ' must be real-valued for all $0 \le \theta < \pi$, the argument of the arccos function cannot be allowed to go beyond unity in magnitude. Hence,

$$\frac{\alpha + \max\limits_{\theta} \mathrm{j}\ln\left(\frac{\mathrm{e}^{-\mathrm{j}kd\cos\theta} - \zeta}{1 - \zeta\mathrm{e}^{-\mathrm{j}kd\cos\theta}}\right)}{kd'} \le 1, \tag{51}$$

and also

$$\frac{\alpha + \min\limits_{\theta} \mathrm{j}\ln\left(\frac{\mathrm{e}^{-\mathrm{j}kd\cos\theta} - \zeta}{1 - \zeta\mathrm{e}^{-\mathrm{j}kd\cos\theta}}\right)}{kd'} \ge -1. \tag{52}$$

For each angle θ there is another angle $\tilde{\theta}$, for which the cosine function returns a value of the same magnitude but of opposite sign. From (50) it is clear that changing the sign of the cosine function results in a complex conjugation (for ζ is real-valued) and thus in a change of the sign of the angle. Therefore,

$$\max_{\theta} \mathrm{j}\ln\left(\frac{\mathrm{e}^{-\mathrm{j}kd\cos\theta} - \zeta}{1 - \zeta\mathrm{e}^{-\mathrm{j}kd\cos\theta}}\right) = -\min_{\theta} \mathrm{j}\ln\left(\frac{\mathrm{e}^{-\mathrm{j}kd\cos\theta} - \zeta}{1 - \zeta\mathrm{e}^{-\mathrm{j}kd\cos\theta}}\right). \tag{53}$$

Using this result in (52) leads with the help of (51) to

$$kd' \ge |\alpha| + \max_{\theta} \mathrm{j}\ln\left(\frac{\mathrm{e}^{-\mathrm{j}kd\cos\theta} - \zeta}{1 - \zeta\mathrm{e}^{-\mathrm{j}kd\cos\theta}}\right). \tag{54}$$

While the separation d' of the virtual isotrops is a logical parameter that can be set rather freely and independently from the separation d of the physical antennas, we see from (54) that there is a *minimum allowable separation* of the virtual isotrops. In order to have this minimum allowable separation as small as possible, one should choose

$$\alpha = 0, \tag{55}$$

resulting in

$$kd' \ge \max_{\theta} \mathrm{j}\ln\left(\frac{\mathrm{e}^{-\mathrm{j}kd\cos\theta} - \zeta}{1 - \zeta\mathrm{e}^{-\mathrm{j}kd\cos\theta}}\right), \tag{56}$$

and

$$\theta' = \arccos\left(\frac{\mathrm{j}}{kd'}\ln\left(\frac{\mathrm{e}^{-\mathrm{j}kd\cos\theta} - \zeta}{1 - \zeta\mathrm{e}^{-\mathrm{j}kd\cos\theta}}\right)\right). \tag{57}$$

Now it turns out that for $kd \ge \pi$, the maximum in (56) is π, such that then $kd' \ge \pi$. In the case $kd < \pi$, the maximum is less than π and it occurs at $\theta = 0$. In total, we find:

$$d' \ge d'_{\min}, \tag{58}$$

where

$$d'_{\min} = \begin{cases} \dfrac{\mathrm{j}}{k}\ln\left(\dfrac{\mathrm{e}^{-\mathrm{j}kd} - \zeta}{1 - \zeta\mathrm{e}^{-\mathrm{j}kd}}\right) & \text{for } kd < \pi, \\ \dfrac{\pi}{k} & \text{for } kd \ge \pi. \end{cases} \tag{59}$$

The value of ζ which must be used depends on kd and can be taken from Figure 2. Figure 4 shows the resulting minimum allowable separation $d'_{\min}/\lambda$ of the virtual isotrops as a function of the separation d/λ of the physical antennas. As long as the physical antennas are spaced at least half a wavelength apart, the virtual isotrops' separation can be anything larger than or equal to half a wavelength. However, as the physical array becomes smaller than half a wavelength, we see that $d'_{\min}$ begins to drop monotonically approaching a finite value as $d/\lambda \to 0$. This value is obtained by using (44) in (59) and then taking the limit $kd \to 0$:

$$\lim_{kd\to 0} \mathrm{j}\ln\left(\frac{\mathrm{e}^{-\mathrm{j}kd} - 1 + kd/\tau}{1 - (1 - kd/\tau)\mathrm{e}^{-\mathrm{j}kd}}\right) = \pi - 2\arctan\frac{1}{\tau} = \tau. \tag{60}$$

The last equality follows with the help of (45) and the fact that $1/\tan(x) = \tan(\pi/2 - x)$. Therefore, we obtain

$$\lim_{kd \to 0} \; d'_{\min} = \frac{\tau}{2\pi}\lambda \approx 0.371\lambda. \tag{61}$$

In any circumstance, the size d' of the virtual array of isotrops must stay above about 0.371λ, while the true physical array may become arbitrarily small. Note that if one decides to make the virtual array of isotrops nevertheless smaller than 0.371λ, then some of the angles θ which the physical array sees would have no real representation for the virtual array, because some real-valued θ would be mapped by (57) to imaginary-valued θ'.

Figure 5 shows an example of the angle transformation (57) which is obtained from setting $d = \lambda/8$, and $d' = 3\lambda/8$. Note that the angles $\theta \in \{0, 90°, 180°\}$ are mapped onto themselves. Yet, two lines which make an angle of $\Delta\theta = 10°$ around $\theta = 90°$ from the physical array's point of view, will make an almost twice as large angle of $\Delta\theta' \approx 19°$ from the viewpoint of the virtual array of isotrops. This follows from the higher than unity slope of θ' with respect to θ around $\theta = 90°$, as is apparent in Figure 5. On the other hand, if the physical array sees the same angle spread of $\Delta\theta = 10°$ centered around $\theta = 160°$, the virtual array of isotrops will now see a much smaller angle spread of about $\Delta\theta' \approx 6.2°$ which is centered around $\theta' \approx 168°$. This means that the virtual array of isotrops faces a *distorted geometrical situation* compared to the real physical array. Both the angle spreads and the center angles are substantially different for the physical and the virtual array.

VII. Summary and Discussion

We have started with an array of two physical non-isotropic antennas which are separated by a distance d and each have a very specific beam-pattern given in (40), and which we repeat for convenience:

$$|g(\theta)|^2 = \frac{1-\zeta^2}{1+\zeta^2} \cdot \frac{1-\zeta^2}{1+\zeta^2-2\zeta\cos\left(kd\cos\theta\right)}. \tag{62}$$

The factor ζ also depends on d and has to be chosen according to Figure 2. Examples of the resulting beam-patterns are displayed in Figure 3. Due to their spatial proximity the antennas experience electromagnetic mutual coupling. This leads to the fact that the radiated power is computed according to (11) as

$$P_{\text{rad}} = R\, \boldsymbol{i}_{\text{A}}^{\text{H}} \begin{bmatrix} 1 & a \\ a & 1 \end{bmatrix} \boldsymbol{i}_{\text{A}}, \quad R > 0,$$

where the mutual coupling coefficient, a, depends both on the separation d and the beam-pattern $|g(\theta)|^2$ of the antennas, and is given explicitly in (12). The electric field strength $\mathcal{E}$ in a point in the far-field and the received power is given by (8):

$$\mathcal{E} = \alpha \left|\boldsymbol{i}_{\text{A}}^{\text{T}} \boldsymbol{a}(\theta)\right|/r, \quad P_{\text{rec}} \sim \left|\boldsymbol{i}_{\text{A}}^{\text{T}} \boldsymbol{a}(\theta)\right|^2, \tag{63}$$

where the last equation assumes that the received power is proportional to the square of the electric field strength, as it usually is in the far-field. The array steering vector $\boldsymbol{a}(\theta)$ is defined in (1) as

$$\boldsymbol{a}(\theta) = g(\theta) \begin{bmatrix} 1 \\ \mathrm{e}^{-\mathrm{j}kd\cos\theta} \end{bmatrix}.$$

Now the antenna excitation ports are decoupled by means of a loss-less linear decoupling 4-port. Calling $\boldsymbol{i}$ the excitation current vector at the decoupled ports, the radiated power is now given by (15) as

$$P_{\text{rad}} = R\, \boldsymbol{i}^{\text{H}} \boldsymbol{i}. \tag{64}$$

Moreover, the electric field strength and received power can be given equivalently to (63) as

$$\mathcal{E} = \alpha \left|\boldsymbol{i}^{\text{T}} \boldsymbol{a}'(\theta')\right|/r, \quad P_{\text{rec}} \sim \left|\boldsymbol{i}^{\text{T}} \boldsymbol{a}'(\theta')\right|^2, \tag{65}$$

where the new steering vector is given from (18) and (36) as:

$$\boldsymbol{a}'(\theta') = \begin{bmatrix} 1 \\ \mathrm{e}^{-\mathrm{j}kd'\cos\theta'} \end{bmatrix}. \tag{66}$$

The equations (64), (65) and (66) describe a virtual array of two uncoupled isotropic radiators separated by the distance d'. However, in order that (65) is indeed identical with (63) one must accept a non-linear distortion of the geometry between the physical and the virtual array according to (57):

$$\theta' = \arccos\left(\frac{\mathrm{j}}{kd'}\ln\left(\frac{\mathrm{e}^{-\mathrm{j}kd\cos\theta} - \zeta}{1 - \zeta\mathrm{e}^{-\mathrm{j}kd\cos\theta}}\right)\right).$$

The factor ζ is the same as the one used in the beam-pattern (62) and must be taken according to Figure 2. The effect of geometric distortion is visualized in Figure 5. One consequence of this unavoidable distortion of geometry is that in *every circumstance, the distance d' of the virtual array of uncoupled isotrops must be chosen larger than or at least equal to a well-defined lower limit:*

$$d' \geq \frac{\tau}{2\pi}\lambda \;\approx\; 0.371\lambda. \tag{67}$$

We remark that this constraint on the separation of the virtual isotrops opens up a path to a novel explanation of the mutual coupling effects on multi-antenna system performance. Recently, it was shown that the presence of mutual coupling in *compact* antenna arrays can lead to surprisingly good multi-streaming capabilities [4], [5], high diversity [6] and a large region of achievable rates in a Gaussian multiple access scenario [7], despite the close proximity of the antennas inside the arrays. Using the just developed model of a virtual array of uncoupled isotrops, it is easy to understand these results qualitatively. At first, one does not have to worry about mutual coupling, for the virtual array's isotrops are uncoupled. However, because of (67) we see that the aperture d' of our virtual array must be quite substantial even though the real physical array which it models might be arbitrarily compact. The relatively large size $d' \geq 0.371\lambda$ of the virtual array makes it understandable that multi-streaming, diversity and multi-user operations may well be carried out perfectly despite the compact antenna spacing of the real physical system which is being modeled. In other words, *the developed model of a virtual array of uncoupled isotrops provides a novel geometrical interpretation of the effect of mutual antenna coupling by representing the latter by constraints on the virtual antenna separation and by a certain distortion of geometrical angles.*

Let us now look into an illustrative example. The physical array's antennas should be placed the distance $d = \lambda/8$ apart:

$$d = \lambda/8 \quad \longrightarrow \quad \zeta = 1/\sqrt{2}.$$

Using this value for ζ in (62), we obtain the beam-pattern that each of the physical antennas *must* have:

$$|g(\theta)|^2 = \frac{1}{9 - 6\sqrt{2}\cos\left(\frac{\pi}{4}\cos\theta\right)}.$$

The pattern has its maximum in front-fire direction ($\theta = \pi/2$). Its value equals the directivity

$$D = \frac{1}{9 - 6\sqrt{2}} \approx 1.94,$$

or 2.88 dB. Hence, each of the individual physical antennas must produce a 1.94 times larger power density in the front-fire direction, than an isotropic radiator would if it radiated the same power. On the other hand, in the end-fire direction ($\theta \in \{0, \pi\}$) exactly 1/3 of the power density is generated compared to isotropically radiating the same power, that is, about 4.77 dB less. Using the value $\zeta = 1/\sqrt{2}$ in (33), we obtain for the mutual coupling coefficient $a = 2\sqrt{2}/3 \approx 0.943$. Now let us turn to the virtual array of uncoupled isotrops, which is accessed by the two decoupled ports of the decoupling 4-port. Setting $\beta = \pi/2$, we obtain with (55), (16) and (34) the electric current transformation:

$$\begin{bmatrix} i_{A,1} \\ i_{A,2} \end{bmatrix} = \mathrm{j} \begin{bmatrix} \sqrt{6} & -\sqrt{3} \\ -\sqrt{3} & \sqrt{6} \end{bmatrix} \begin{bmatrix} i_1 \\ i_2 \end{bmatrix}.$$

If we make $i_2 = 0$, then $i_{A,1} = \mathrm{j}\sqrt{6} i_1$, and $i_{A,2} = -\mathrm{j}\sqrt{3} i_1$, such that both physical antennas are driven with different currents. Together with the carefully chosen beam-pattern of the individual physical antennas, this results in an exact isotropic radiation. *Driving only one of the decoupled ports with a non-zero current, results in isotropic radiation.* This follows immediately from (65) and (66). What is the spacing of the virtual antennas? From (59), we see that $d'_{\min} = \frac{3}{8}\lambda$. We choose for our virtual array of isotrops this minimum separation

$$d' = \frac{3\lambda}{8}.$$

Note that the real physical array is then exactly 3 times smaller than our virtual array of uncoupled isotrops. The virtual array, however, not just has different size from the physical array, it also has a *distorted geometry*, because it perceives the angles differently than the physical array. The mapping between the physical array's elevation angle θ, and the virtual array's elevation angle θ' can be evaluated from (57). Figure 5 shows this relationship. The virtual array is more sensitive for directions around the front-fire, because

$$\left.\frac{\mathrm{d}\theta'}{\mathrm{d}\theta}\right|_{\theta=\pi/2} = \frac{1}{9 - 6\sqrt{2}} \approx 1.94.$$

It is interesting enough, that this is exactly the same number as the maximum directivity of each individual element of the physical array. In the end-fire direction, the virtual array is less sensitive:

$$\left.\frac{\mathrm{d}\theta'}{\mathrm{d}\theta}\right|_{\theta=0} = \frac{1}{\sqrt{3}} \approx 0.577.$$

A small angle-spread in the real-world is perceived by the virtual array by the factor 1.94 larger when it comes from the front-fire direction, while the same angle-spread in the real-world is perceived by the factor $\sqrt{3}$ smaller by the virtual array when it comes from the end-fire direction. This is why there is an unavoidable distortion of the geometric picture of the propagation channel. Let us now try to excite the virtual array. For example, we choose:

$$\boldsymbol{i} = \begin{bmatrix} \sqrt{3} \\ \mathrm{j}\sqrt{6} \end{bmatrix} \mathrm{A}.$$

The decoupling 4-port converts this into the excitation of the physical array:

$$\boldsymbol{i}_A = 3\mathrm{A} \begin{bmatrix} (1+\mathrm{j})\sqrt{2} \\ -2-\mathrm{j} \end{bmatrix}.$$

How much power is radiated?

$$P_{\mathrm{rad}} = R\,\boldsymbol{i}^{\mathrm{H}}\boldsymbol{i} = R\,\boldsymbol{i}_A^{\mathrm{H}} \begin{bmatrix} 1 & 2\sqrt{2}/3 \\ 2\sqrt{2}/3 & 1 \end{bmatrix} \boldsymbol{i}_A = R \cdot 9\,\mathrm{A}^2.$$

Now let us see how much electric field strength is produced in a distance r in the far-field in the direction $\theta = 45°$, as seen by the *physical* array. From the *virtual* array's point of view, the angle is $\theta' \approx 29.14°$. The virtual array's steering vector then becomes:

$$\boldsymbol{a}'(29.14°) = \begin{bmatrix} 1 \\ \mathrm{e}^{-\mathrm{j}(3\pi/4)\cos 29.14°} \end{bmatrix} \approx \begin{bmatrix} 1 \\ \mathrm{e}^{-\mathrm{j}2.05798} \end{bmatrix}.$$

The square of the electric field strength then computes as

$$\mathcal{E}^2 = |\alpha|^2 \left|\boldsymbol{i}^{\mathrm{T}}\boldsymbol{a}'(29.14°)\right|^2 / r^2 \approx 16.5|\alpha|^2/r^2.$$

Calculating the same thing from the physical array's viewpoint, we need to now the steering vector in the direction $\theta = 45°$:

$$|g(45°)|^2 \approx 0.55867, \quad \boldsymbol{a}(45°) \approx \begin{bmatrix} 1 \\ \mathrm{e}^{-\mathrm{j}(\pi/4)\cos 45°} \end{bmatrix} \sqrt{0.55867}.$$

Then the square of the electric field strength computes as

$$\mathcal{E}^2 = |\alpha|^2 \left|\boldsymbol{i}_A^{\mathrm{T}}\boldsymbol{a}(45°)\right|^2 / r^2 \approx 16.5|\alpha|^2/r^2.$$

As it should, the result is the same as when computed from the virtual array's point of view.

VIII. The Loss-Less Decoupling 4-Port

Up to now it was just assumed that a loss-less 4-port really exists, which will produce the right electric current transformation matrix $\boldsymbol{T}$ from (34), which becomes with (55):

$$\boldsymbol{T} = \mathrm{e}^{\mathrm{j}\beta} \frac{\sqrt{1+\zeta^2}}{1-\zeta^2} \begin{bmatrix} 1 & -\zeta \\ -\zeta & 1 \end{bmatrix}, \tag{68}$$

where $\beta \in \mathbb{R}$, and ζ is taken from Figure 2. Furthermore, it has to decouple the physical antenna array's excitation ports such that they look as individual resistors of value R. The

ports of the physical antenna array can be described by their impedance matrix $\boldsymbol{Z}_\mathrm{A}$, such that

$$\boldsymbol{u}_\mathrm{A} = \boldsymbol{Z}_\mathrm{A}\boldsymbol{i}_\mathrm{A}, \tag{69}$$

where $\boldsymbol{u}_\mathrm{A}$ is the vector of the voltages that appear across the physical array's excitation ports. Assuming the antennas are loss-less, the power which enters the antenna excitation ports is radiated, hence:

$$P_\mathrm{rad} = \mathrm{Re}\{\boldsymbol{u}_\mathrm{A}^\mathrm{H}\boldsymbol{i}_\mathrm{A}\} = \boldsymbol{i}_\mathrm{A}^\mathrm{H}\,\mathrm{Re}\{\boldsymbol{Z}_\mathrm{A}\}\,\boldsymbol{i}_\mathrm{A}. \tag{70}$$

This comes about because antennas are reciprocal which requires that $\boldsymbol{Z}_\mathrm{A} = \boldsymbol{Z}_\mathrm{A}^\mathrm{T}$. Comparing (70) with (11) it follows that

$$\mathrm{Re}\{\boldsymbol{Z}_\mathrm{A}\} = R\begin{bmatrix}1 & a\\ a & 1\end{bmatrix}, \tag{71}$$

where a is the mutual coupling coefficient. Let the decoupling 4-port also be described by an impedance matrix:

$$\begin{bmatrix}\boldsymbol{u}\\ \boldsymbol{u}_\mathrm{A}\end{bmatrix} = \mathrm{j}\begin{bmatrix}\boldsymbol{A} & \boldsymbol{B}^\mathrm{T}\\ \boldsymbol{B} & \boldsymbol{C}\end{bmatrix}\begin{bmatrix}\boldsymbol{i}\\ -\boldsymbol{i}_\mathrm{A}\end{bmatrix}, \tag{72}$$

where $\boldsymbol{u}$ and $\boldsymbol{i}$ are voltage and current vectors of the two decoupled ports, and the matrices $\boldsymbol{A}$, $\boldsymbol{B}$ and $\boldsymbol{C}$ are real-valued, with $\boldsymbol{A}$ and $\boldsymbol{C}$ also being symmetric. Thus, the decoupling 4-port is *reciprocal* and *lossless* [8]. From (69) and the second row of (72) we have with $\boldsymbol{i}_\mathrm{A} = \boldsymbol{T}\boldsymbol{i}$ that

$$\boldsymbol{T} = \mathrm{j}\,(\boldsymbol{Z}_\mathrm{A} + \mathrm{j}\boldsymbol{C})^{-1}\boldsymbol{B}. \tag{73}$$

Now let us choose

$$\boldsymbol{C} = -\mathrm{Im}\{\boldsymbol{Z}_\mathrm{A}\}, \quad \boldsymbol{B} = b\,\mathrm{Re}\{\boldsymbol{Z}_\mathrm{A}\}^{1/2}, \tag{74}$$

where $b \in \mathbb{R}\cdot\sqrt{\mathrm{V/A}}$, is a constant to be determined. Substituting (74) into (73), we find:

$$\boldsymbol{T}^2 = -b^2\,\mathrm{Re}\{\boldsymbol{Z}_\mathrm{A}\}^{-1} = -\frac{b^2}{R}\frac{1}{1-a^2}\begin{bmatrix}1 & -a\\ -a & 1\end{bmatrix}, \tag{75}$$

where the last equality comes with the help of (71). With the right-most term of (33) it follows:

$$\boldsymbol{T}^2 = -\frac{b^2}{R}\frac{1+\zeta^2}{(1-\zeta^2)^2}\begin{bmatrix}1+\zeta^2 & -2\zeta\\ -2\zeta & 1+\zeta^2\end{bmatrix}. \tag{76}$$

On the other hand, from (68) we must have

$$\boldsymbol{T}^2 = \mathrm{e}^{2\mathrm{j}\beta}\frac{1+\zeta^2}{(1-\zeta^2)^2}\begin{bmatrix}1+\zeta^2 & -2\zeta\\ -2\zeta & 1+\zeta^2\end{bmatrix}. \tag{77}$$

Comparing (76) with (77) then shows that

$$\mathrm{e}^{2\mathrm{j}\beta} = -\frac{b^2}{R}, \tag{78}$$

must hold true. Because b^2 and R are real-valued and non-negative, it follows

$$\beta = \pm\pi/2, \quad b = \pm\sqrt{R}. \tag{79}$$

Thus,

$$\boldsymbol{T} = \pm\mathrm{j}\frac{\sqrt{1+\zeta^2}}{1-\zeta^2}\begin{bmatrix}1 & -\zeta\\ -\zeta & 1\end{bmatrix}. \tag{80}$$

From the first line of (72) and $\boldsymbol{i}_\mathrm{A} = \boldsymbol{T}\boldsymbol{i}$, it follows with (73) that

$$\boldsymbol{u} = \left(\mathrm{j}\boldsymbol{A} + \boldsymbol{B}^\mathrm{T}\,(\boldsymbol{Z}_\mathrm{A} + \mathrm{j}\boldsymbol{C})^{-1}\boldsymbol{B}\right)\boldsymbol{i}. \tag{81}$$

Substituting (74) with $b = \pm\sqrt{R}$ from (79) then yields

$$\boldsymbol{u} = \left(\mathrm{j}\boldsymbol{A} + R\,\mathbf{I}\right)\boldsymbol{i}, \tag{82}$$

where $\mathbf{I}$ is the identity matrix. In order to obtain $\boldsymbol{u} = R\boldsymbol{i}$, and thereby ensure that the ports are decoupled, all we have to do is to set:

$$\boldsymbol{A} = \mathbf{O}, \tag{83}$$

where $\mathbf{O}$ denotes the all zeros matrix. Therefore, with $\boldsymbol{A} = \mathbf{O}$, $\boldsymbol{B} = \pm\sqrt{R}\mathrm{Re}\{\boldsymbol{Z}_\mathrm{A}\}^{1/2}$, and $\boldsymbol{C} = -\mathrm{Im}\{\boldsymbol{Z}_\mathrm{A}\}$, the parameters of the reciprocal and loss-less matching 4-port are defined. It implements both the desired electric current transformation matrix (80), and decouples the output ports making them look like positive resistances of value R.

IX. Conclusion

We have analyzed to what extent the model of an array of two uncoupled isotropic radiators can make physical sense. This is indeed possible in the sense of a *virtual* antenna array which is obtained from a real physical array and a loss-less decoupling network. For this to work out, it is necessary that 1) the antennas of the *real* physical array are *not* isotrops at all, but have a carefully chosen beam-pattern which we have derived in closed-form, 2) the model distance between the antennas of the virtual array is chosen large enough so that it is kept above a well-defined lower bound of about 0.371 times the wavelength, and 3) one has to accept a distortion of the geometry between the real physical array and the virtual array of uncoupled isotrops, which leads to a non-linear relationship between the geometrical angles that are observed by the physical and the virtual array, respectively. These constraints on separation and distortion of angles makes for a novel geometrical representation of the effect of mutual antenna coupling. This geometrical representation makes it easy to qualitatively understand the effect of mutual coupling on multi-streaming, diversity and multi-user performance of compact antenna radio communication systems.

References

[1] H. Yordanov, M. T. Ivrlač, P. Russer, and J. A. Nossek, "Arrays of Isotropic Radiators — A Field-theoretic Justification," in *ITG International Workshop on Smart Antennas*, Berlin, Germany, feb 2009.

[2] D. Tse and P. Viswanath, *Fundamentals of Wireless Communication*. Cambridge University Press, 2005.

[3] A. Balanis, *Antenna Theory*. Second Edition, John Wiley & Sons, 1997.

[4] M. Ivrlač and J. Nossek, "On Multistreaming with Compact Antenna Arrays," in *Proc. ITG International Workshop on Smart Antennas*, 2011, pp. 1–8.

[5] M. T. Ivrlač and J. A. Nossek, "Toward a Circuit Theory of Communication," *IEEE Transactions on Circuits and Systems I: Regular Papers*, vol. 57(7), pp. 1663–1683, 2010.

[6] M. Ivrlač and J. Nossek, "On the Diversity Performance of Compact Antenna Arrays," in *Proc. of the 30th General Assembly of the International Union of Radio Science (URSI)*, 2011, p. (in press).

[7] ——, "Gaussian Multiple Access Channel with Compact Antenna Arrays," in *Proc. of the IEEE International Symposium on Information Theory (ISIT)*, 2011, pp. 728–731.

[8] V. Belevitch, *Classical Network Theory*. Holden Day, San Francisco, 1968.